Simulating infrared limb radiances from MIPAS in the ECMWF system

Niels Bormann, Sean Healy, Marco Matricardi, and Frédéric Chevallier

ECMWF, Shinfield Park, Reading
RG2 9AX, United Kingdom
n.bormann@ecmwf.int

ABSTRACT

A new fast radiative transfer model to compute infrared limb radiances for the Michelson Interferometer for Passive Atmospheric Sounding (MIPAS) has been developed and validated, and a first application is presented. The model, referred to as RTMIPAS, can simulate radiances for all channels of the high-spectral resolution MIPAS instrument in the 685-2000 cm^{-1} wavenumber region. RTMIPAS is part of a wider effort to develop the capability to assimilate infrared limb radiances into the ECMWF model. The model uses the regression-based methodology of RTTOV, and it can simulate the effect of variable water vapour and ozone; for other gases included in the model a fixed climatological profile is assumed.

RTMIPAS can reproduce line-by-line radiances to an accuracy that is below the noise-level of the instrument for most spectral points and tangent heights, while offering significantly more rapid radiance calculations compared to currently available radiative transfer models. The comparison of RTMIPAS transmittances with line-by-line model equivalents indicates that the accuracy of the RTMIPAS transmittance model is comparable to that of similar regression-based radiative transfer models for the Earth-looking geometry.

Preliminary experiments with simulated data in a 1-dimensional variational analysis scheme highlight the potential of MIPAS data to considerably reduce analysis errors in the stratosphere. Issues to be addressed for work with real data are also discussed.

1 Introduction

This contribution describes the development, validation and a first application of a new fast radiative transfer model for limb radiances from the Michelson Interferometer for Passive Atmospheric Sounding (MIPAS) on-board the Envisat satellite (e.g., European Space Agency, ESA, 2000) . These are the first steps of a wider effort to assimilate infrared limb radiances into a numerical weather prediction (NWP) model. MIPAS is a very high spectral resolution interferometer (0.025 cm^{-1}, unapodised), measuring infrared limb radiances in 5 spectral bands between 685 and 2410 cm^{-1} (Table 1), providing a total of 59,605 spectral points (i.e., channels). MIPAS is designed to provide information on the thermal structure and chemical composition of the upper troposphere and the stratosphere at high vertical resolution.

The new fast radiative transfer model is referred to as RTMIPAS, and it is based on methodology developed for the RTTOV fast radiative transfer model for nadir[1] looking geometry (e.g., Matricardi *et al.* 2004, Eyre 1991). In RTTOV, the atmosphere is represented on fixed pressure levels, and convolved level-to-space transmittances are calculated based on linear regression models for the effective layer optical depths. The linear regressions are derived from a large transmittance database from line-by-line (LBL) radiative transfer computations. In the current version of RTMIPAS, only water vapour and ozone are treated as variable gases, but the method could be extended to other gases if required. The RTTOV approach is used for the direct assimilation of nadir radiances at ECMWF and a number of other NWP centres.

[1] In the following, the term "nadir" is used to refer to the Earth-looking geometry in general, rather than a view with a zenith angle of 0° only.

Table 1: Main characteristics of MIPAS.

Spectral resolution	0.025 cm^{-1}, unapodised (0.035 cm^{-1}, apodised)		
Spectral bands	A-band:	685-970 cm^{-1}	(11,401 spectral points)
	AB-band:	1020-1170 cm^{-1}	(6,001 spectral points)
	B-band:	1215-1500 cm^{-1}	(11,401 spectral points)
	C-band:	1570-1750 cm^{-1}	(7,201 spectral points)
	D-band:	1820-2410 cm^{-1}	(23,601 spectral points)
Nominal tangent altitudes in normal scanning mode	6-42 km in 3 km steps; 47, 52, 60, 68 km.		
Field of view at tangent point (vertical $\times$ horizontal)	approximately 3 km $\times$ 30 km		

The structure of this paper is as follows: first, we summarise RTMIPAS-specific modifications of the RTTOV method for the radiative transfer parameterisations. We then evaluate the performance of the scheme compared to LBL computations, before preliminary experiments with a 1-dimensional variational (1DVAR) scheme are presented. Conclusions are drawn in the last section in which we also give an overview of outstanding issues.

2 Description of the fast model

For a detailed description of the RTTOV methodology the reader is referred to Matricardi and Saunders (1999). Here, we will briefly summarise the RTMIPAS-specific implementation choices, and a more detailed description can be found in Bormann *et al.* (2004).

In RTMIPAS, the radiative transfer equation is solved numerically based on 81 fixed pressure levels. No surface term is needed in the case of the limb geometry. The pressure levels are given in Bormann *et al.* (2004) and displayed in Figure 1. The spacing of the levels is similar to that used by Matricardi (2003), and it has been chosen by taking into account typical temperature lapse rates and the expected future vertical resolution of the ECMWF forecast model. As in RTTOV, linear regression models for suitable predictors are used to compute effective channel optical depths for each layer defined by the given discretisation. Only water vapour and ozone are treated as variable gases, whereas contributions from all other relevant gases are based on fixed climatological profiles (John Remedios 2003, pers. communication).

In the limb geometry, ray tracing is required to obtain the ray path and the atmospheric conditions along the path for a given atmospheric state and the satellite's pointing information. Note that a given ray will not necessarily cross all the layers introduced in RTMIPAS, and the ones which are crossed are crossed twice (Fig. 1). As a result, regressions for the effective layer optical depths for $N = 160$ layers are required. The ray tracing is performed using the methods of Healy and Eyre (2003). We consider only such rays whose tangent heights lie on the 34 selected layer boundaries indicated in Fig. 1, and we use the field of view convolution described below to calculate the radiances for any other tangent height viewed by MIPAS. The hydrostatic equation is used to obtain the geometric height if it is not provided by the user.

The predictors used in the transmittance parameterisation have been specifically developed for the limb geometry, and they are discussed in detail in Bormann *et al.* (2004). The predictors are originally based on Matricardi (2003), and a necessary first adjustment was to replace the secant of the satellite zenith angle with the actual layer path length.

The transmittance database used to derive the regression coefficients for RTMIPAS was generated using the Reference Forward Model (RFM; Dudhia *et al.* 2002b). Line data were taken from the 2000 edition of the

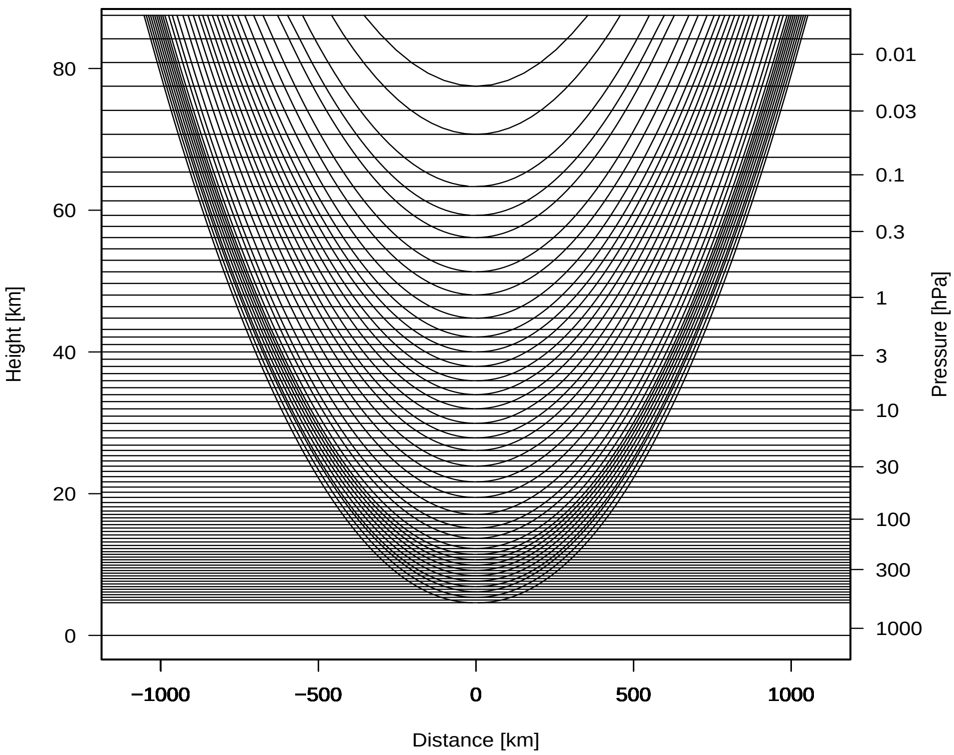

Figure 1: Schematic representation of the levels (horizontal lines) and pencil beams (curved lines) used in RTMIPAS, mapped into a plane-parallel view. An atmospheric mean profile has been used to convert the RTMIPAS pressure levels to heights.

HITRAN molecular database. As in RTIASI, a separate parameterisation is used for the water vapour continuum, based on the CKD 2.4 continuum model (Clough *et al.* 1989). Monochromatic LBL calculations were performed at a resolution of 0.0005 cm^{-1}. These high-resolution spectra were subsequently convolved with the MIPAS ILSs, apodised using Norton-Beer strong apodisation (Didem Alpaslan and Rob Koopmann 2003, pers. communication). Note that we consider only MIPAS channels in the wavenumber range 685-2000 cm^{-1}, as the channels in the 2000-2410 cm^{-1} region of the spectrum are contaminated by solar radiation and also show a low signal-to-noise ratio.

The LBL computations were performed for a set of 46 diverse atmospheric profiles, assuming horizontal homogeneity in the calculations. The profiles were sampled from the 60 level ERA-40 reanalysis (e.g., Simmons and Gibson 2000) using the method of Chevallier (2002), maximising the variability in the stratosphere and upper troposphere above 550 hPa. The profiles provide thermodynamically consistent values of pressure, temperature, and mixing ratios for water vapour and ozone. The number of profiles used in the training set is comparable to that typically used in the derivation of regression coefficients for fast models for the nadir viewing geometry, such as in Matricardi *et al.* (2004).

One added complexity in radiative transfer models for MIPAS is that the FOV convolution in the vertical has to be taken into account. This requires the computation of radiances for rays with infinitesimal FOV ("pencil beams") over a range of tangent heights, and the subsequent convolution of the radiance versus tangent height relationship with the instrument's normalised FOV function. In RTMIPAS, we found it sufficient to calculate pencil beam radiances for the tangent heights indicated in Fig. 1 only, and then evaluate the FOV integral based on a cubic fit to the radiance profile. Similar approaches are used for the operational ESA retrievals.

3 Validation of the fast model

In this section we study the accuracy of RTMIPAS by comparing pencil beam radiances and transmittances from RTMIPAS with RFM equivalents for the dependent profile set and for a set of profiles independent of the regression coefficients. Note that we validate RTMIPAS against results from the same LBL model used in the training phase, thus characterising the "fast model errors" only, i.e., the errors introduced through the fast transmittance parameterisation.

3.1 Dependent profile set

For the dependent profile set, RTMIPAS can reproduce the RFM radiance spectra to an accuracy that is below the noise level of the MIPAS instrument for most channels and pencil beams over the range considered by RTMIPAS. Figures 2 and 3 show the standard deviation of the RTMIPAS-RFM radiance differences, normalised by the apodised instrument noise (i.e., error-to-noise ratio). For the noise specification, in-flight values of the well-studied orbit 2081 have been used. For display purposes, we show the maximum and the mean error-to-noise ratio for each 80-channel interval (2 cm^{-1}) for each pencil beam. More than 92% of the channels typically show standard deviations of less than half the instrument noise for each pencil beam (e.g., Fig. 4), with an even better performance for the higher pencil beams. Radiance biases are also usually small (typically less than $\frac{1}{10}$th of the instrument noise), except for the lowest pencil beams (e.g., Fig. 4).

As expected, the performance of RTMIPAS changes with spectral band (Figures 2 to 4). Overall, the MIPAS B- and C-band with strong water vapour absorption show the smallest error-to-noise ratio. This is largely due to the small variability of water vapour in the stratosphere. The AB-band with predominantly ozone absorption shows the poorest statistics, particularly in the regions of strong ozone absorption around 1020-1075 cm^{-1}, or in the 1070-1170 cm^{-1} region at lower tangent heights. Further investigations reveal that these errors are predominantly introduced by the ozone transmittance model in RTMIPAS. Similarly, the fast model errors and biases in the 750-800 cm^{-1} wavenumber region of the A-band are also mainly introduced by the ozone transmittance model. Biases tend to be most pronounced at lower levels in the A- and AB-band (e.g., Fig. 4), whereas the other bands exhibit negligible biases throughout.

Root mean squared (RMS) differences between RTMIPAS and the RFM transmittances are typically around $10^{-4} - 10^{-5}$, and the maximum RMS difference rarely exceeds 0.005 (Fig. 5). The errors are comparable to those found in Matricardi (2003), indicating that the quality of the fast transmittance model in RTMIPAS is comparable to the one for a similar regression-based model for the nadir viewing geometry.

3.2 Independent profile set

We will now characterise the fast model errors for RTMIPAS for an independent set of 53 profiles. As for the training set, this set has been sampled from ERA-40 data, but it provides profiles from atmospheric conditions taken from different times and locations. Note that, as a result of using the same source for sampling the profiles, the independent set may share some statistical characteristics with the training set.

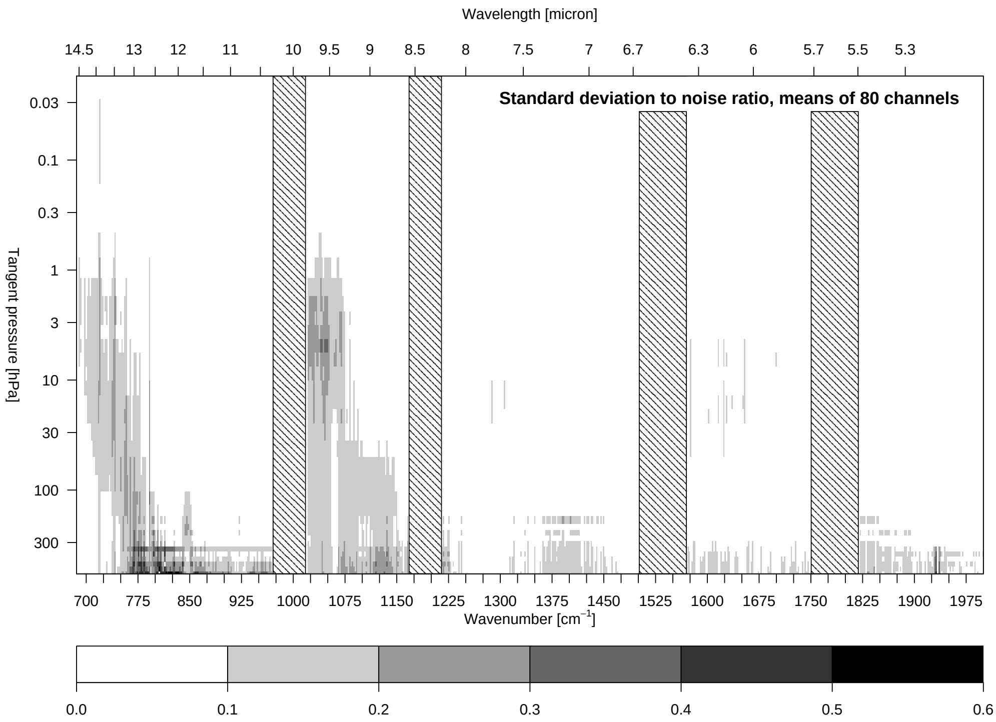

Figure 2: Standard deviation of the RTMIPAS-RFM radiance differences, scaled by the MIPAS noise, for the dependent profile set. The plot shows the mean error to noise ratio over 80-channel intervals (i.e., 2 cm^{-1}) as a function of wavenumber and pencil beam pressure. Spectral regions not covered by MIPAS are hatched.

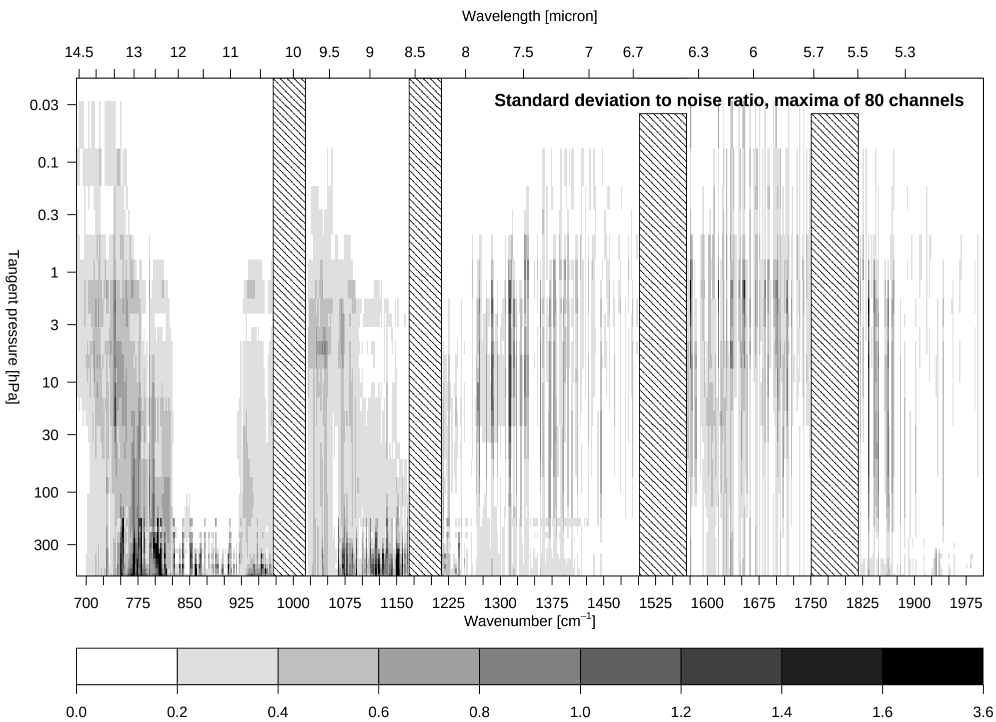

Figure 3: As Fig. 2, but for the maximum error to noise ratio of 80-channel intervals.

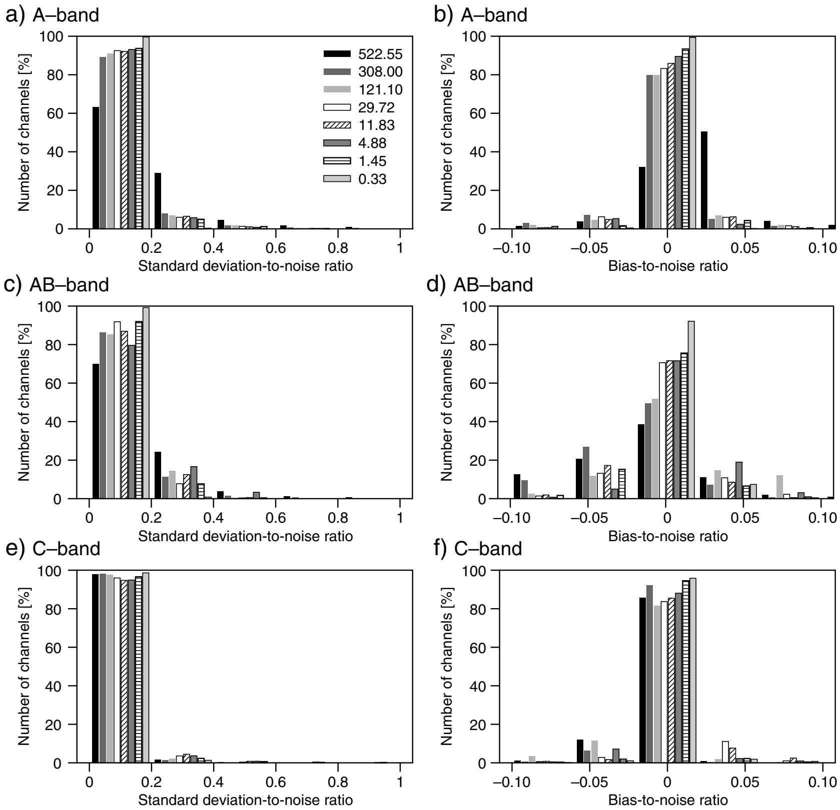

Figure 4: a) Distribution of the number of channels [%] in the MIPAS A-band versus the standard deviation of the RTMIPAS-RFM radiance differences, scaled by the MIPAS noise. The statistic is based on the dependent profile set. Results for 8 selected pencil beams are shown, with their tangent pressures [hPa] indicated in the legend. The binning interval is 0.2. b) As a), but for the mean RTMIPAS-RFM radiance difference, scaled by the MIPAS noise. Binning interval is 0.04. c) As a), but for the MIPAS AB-band. d) As b), but for the MIPAS AB-band. e) As a), but for the MIPAS C-band. f) As b), but for the MIPAS C-band.

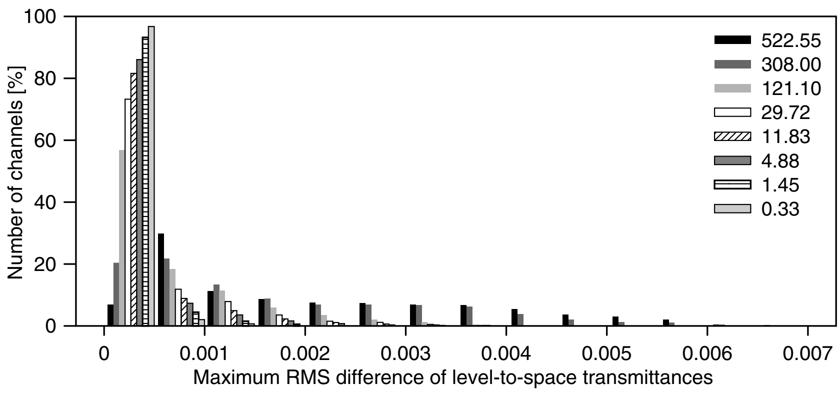

Figure 5: Number of channels [%] versus the channel maximum RMS of the RTMIPAS-RFM differences in the level-to-satellite transmittances. The statistic is based on the dependent profile set. Results for 8 selected pencil beams are shown, with their tangent pressures [hPa] indicated in the legend. The binning interval is $0.5 \cdot 10^{-3}$.

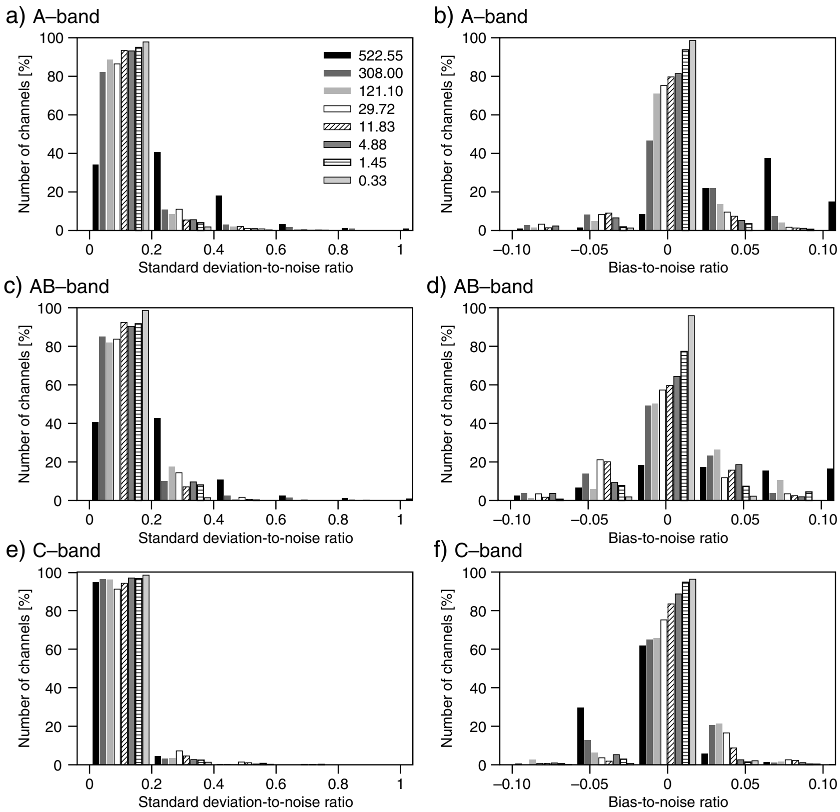

Figure 6: As Fig. 4, but for the independent profile set.

The performance of RTMIPAS for the independent set of profiles is similar to that for the dependent set of profiles, with standard deviations of the RTMIPAS-RFM radiance differences below the noise level of the MIPAS instrument for most channels and pencil beams (cf, Figures 4 and 6). The largest increases in the standard deviation or the mean of the RTMIPAS-RFM differences tend to occur for the lowest pencil beams. Overall, the increase in the errors when moving to the independent profile set is smaller than what is encountered in Matricardi (2003) for the nadir geometry. The similar performance for the independent and the dependent sets of profiles suggests that 46 profiles are adequate for the training of RTMIPAS.

4 Preliminary 1DVAR simulations

To highlight a first application of RTMIPAS we will now present results from some preliminary simulations within a 1DVAR framework. In 1DVAR, we aim to minimise a cost function J of the control vector $\mathbf{x}$ given by,

$$J(\mathbf{x}) = \frac{1}{2}(\mathbf{x}-\mathbf{x}_B)^T\mathbf{B}^{-1}(\mathbf{x}-\mathbf{x}_B) + \frac{1}{2}(H(\mathbf{x})-\mathbf{y})^T\mathbf{R}^{-1}(H(\mathbf{x})-\mathbf{y}) \qquad (1)$$

Here, $\mathbf{x}_B$ denotes the background estimate of the control vector and $\mathbf{y}$ the observations; H is the observation operator, $\mathbf{B}$ the background error covariance matrix and $\mathbf{R}$ the observation error covariance matrix which includes the error covariance for the observation operator. The minimum is found by an iterative process which involves the computation of the gradient of the cost function with respect to the control variable. The latter can be computed using the adjoint of the observation operator. The observation operator in our case is RTMIPAS, and we assume horizontal homogeneity in our simulations to reduce the analysis to a 1-dimensional problem. The 1DVAR scheme used is adapted from Chevallier et al. (2002).

In the following, we perform Monte-Carlo experiments with simulated observations to test the performance of the 1DVAR and to highlight the information that can be extracted from a highly idealised set of MIPAS measurements (similar to Collard and Healy 2003). To generate our "observations" y we used RTMIPAS on a midlatitude daytime reference profile to produce "true" radiance values which were subsequently perturbed by Gaussian noise specified by the apodised instrument error covariance matrix. The resulting "observations" provide 1528 simulated radiance values from 150 selected RTMIPAS channels, taken at up to 17 tangent heights. The control vector x consists of temperature, humidity, and ozone values at the 81 RTMIPAS pressure levels, and the error covariances for the background values x_B have been interpolated from mean ECMWF background error covariances. The background values were obtained by perturbing the midlatitude daytime reference profile with Gaussian noise specified by the background error covariance. We applied the 1DVAR to 500 realisations of these perturbations. Since the true atmospheric state is known in these simulations, we can accumulate error statistics for the resulting 1DVAR analyses.

Figure 7 shows the reduction of the errors in the control vector as a result of using the MIPAS observations in our 1DVAR. It can be seen that the error in all control variables is considerably reduced relative to the background error. Most of the error reduction for temperature is confined to the stratosphere and lower mesosphere above about 30 km. A considerable reduction of the ozone error is visible in the ozone layer. Due to the relatively diagonal background error covariance matrix for ozone, the tangent heights of the MIPAS observations (the regions with the largest information) appear as minima of the analysis error. Mostly, the error estimates obtained in the 1DVAR simulations agree well with estimates calculated from linear theory (Fig. 7). On the one hand this gives confidence in the 1DVAR results, on the other it suggests that linear theory provides an adequate framework for error analysis for MIPAS data.

The above analysis characterises the information content that can be extracted from the selected MIPAS measurements under very idealised conditions given prior information from the ECMWF short-range forecast: the observation and forward model error is unbiased and equal to the instrument error; the background errors are unbiased and as specified; all observations are taken in clear-sky conditions over horizontally homogeneous atmospheres; the pointing information from the satellite is perfectly known; and the height of the lowest level is perfectly known. In reality, the error reduction from the selected channels is thus likely to be lower. However, this may be compensated for by using more MIPAS channels. Our preliminary analysis is thus primarily a

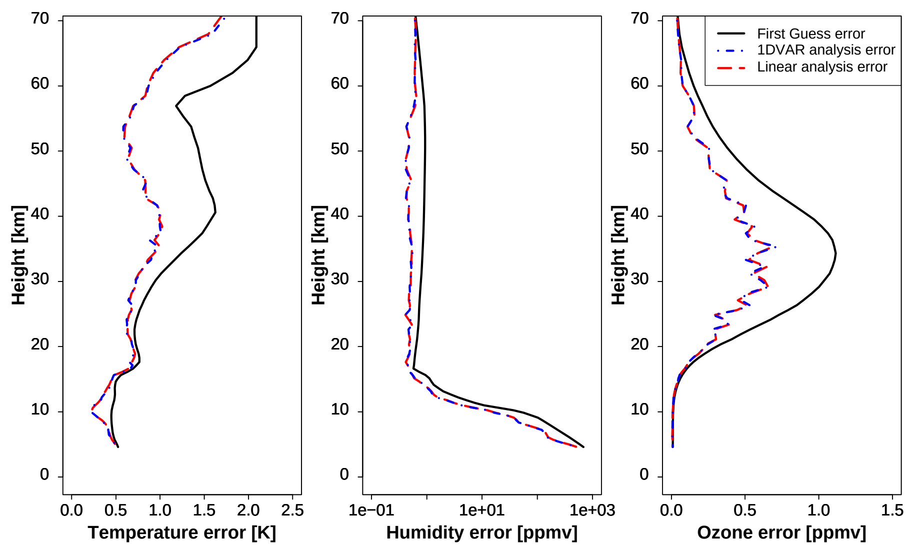

Figure 7: Error analysis from the 1DVAR Monte-Carlo experiments. The solid black line represents the assumed First Guess errors, the blue dash dotted line the analysis errors as calculated from 500 1DVAR simulations, and the red dashed line provides an estimate of the analysis error from linear theory.

qualitative assessment of the MIPAS information content relative to the ECMWF background, and more work is required for a more quantitative analysis.

5 Conclusions and outlook

This paper summarises the development, validation and a first application of a new fast radiative transfer model to compute infrared limb radiances for MIPAS (called RTMIPAS). The model uses similar methodology as RTTOV, and it has been developed with a view to assimilate limb radiances from MIPAS within the ECMWF assimilation system. Tangent linear and adjoint routines have also been developed for use in variational data assimilation.

RTMIPAS can reproduce LBL radiances to an accuracy below the noise-level of the instrument for most spectral points and tangent heights, while offering significantly more rapid calculations compared to currently used radiative transfer methods for the limb geometry. Root mean square differences between the RTMIPAS and the RFM level-to-satellite transmittances are very small, typically around $10^{-4} - 10^{-5}$, and the maximum RMS difference rarely exceeds 0.005 for some pencil beams and channels. This good performance is comparable to that of fast radiative transfer models developed for nadir viewing, based on similar regression-based methodology (e.g., Matricardi 2003). The predictors used in the regression models needed to be adapted from the nadir geometry to limb viewing to achieve this performance, and the final predictor set shows considerable differences to that used in the models for nadir viewing, while the general form of the predictors is similar. The model performs similarly well for the set of training profiles taken from ERA-40 data and an independent set of profiles also sampled from ERA-40 data, suggesting that the model is suitably trained for the expected atmospheric variability. The small errors introduced by the fast transmittance parameterisation in RTMIPAS are not going to give a significant contribution to the total forward model error, compared to uncertainties in the spectroscopy. Preliminary 1DVAR experiments with simulated data highlight the potential of MIPAS data to considerably reduce analysis errors in the stratosphere.

RTMIPAS shows that a regression-based approach to transmittance modelling can be successfully adapted to the limb geometry. The experience with regression-based models for the nadir geometry suggests that the method may be applied to other limb-sounding instruments for the infrared region (such as the High Resolution Dynamics Limb Sounder, HIRDLS), but also for the microwave region (such as the Microwave Limb Sounder, MLS), with little or no changes to the set of predictors used.

For progress towards analyses with real data, either in a 1DVAR framework or within 4DVAR, a number of issues need to be addressed: In limb sounding, the pointing information provided by the satellite is usually not considered accurate enough for quantitative analyses, and instead this information has to be retrieved from the observations. For our purposes, use of the tangent pressure information retrieved in the ESA level 2 product may be an initial solution to this, and approaches to retrieve the tangent height information from the data in a pre-assimilation step or within the main analysis could be explored. Also, methods need to be developed to screen out observations affected by clouds or aerosols which the observation operator currently is unable to deal with. Also, the selection of channels and tangent heights used in our first experiments needs to be revised, for instance by using channel selection methods which iteratively maximise a measure of information content. This step allows to avoid channels with larger RTMIPAS errors, by using channel selection methods which take into account sources of forward model error (e.g., Dudhia *et al.* 2002a). Linked to the channel selection is also the question as to how much benefit could be gained from employing an observation operator which truly reflects the limb geometry and is able to handle horizontal gradients. The error introduced by assuming horizontal homogeneity as in our 1DVAR experiments depends on the characteristics of the selected channels, with channels with weighting functions peaking away from the tangent point introducing the larger errors. The RTMIPAS method is capable of handling horizontal gradients, but more validation work is required in this respect. Another question to be answered during the planned assimilation is whether the current formulation of the background error covariances and the humidity and ozone control variables is adequate to extract stratospheric information from MIPAS radiances directly in a near-optimal way, and what role MIPAS radiances can play in detecting and correcting biases in the background field in the stratosphere.

Acknowledgements

Niels Bormann is funded through the ASSET project (Assimilation of Envisat Data), a shared-cost project co-funded by the Research Directorate General of the European Commission within the activities of the Environment and Sustainable Development sub-programme of the 5th Framework Programme. We thank all ASSET partners for many helpful discussions. Marco Matricardi and Sean Healy are supported by EUMETSAT. We are especially grateful to Anu Dudhia (Oxford University) for making the RFM available and for providing valuable support throughout this project. We thank Anabel Bowen and Rob Hine for preparing some of the Figures.

References

Bormann, N., M. Matricardi, and S. B. Healy, 2004: RTMIPAS: A fast radiative transfer model for the assimilation of infrared limb radiances from MIPAS. Technical Memorandum 436, ECMWF, Reading, UK, 49 pp.

Chevallier, F., 2002: Sampled database of 60-level atmospheric profiles from the ECMWF analyses. NWP SAF Report 4, ECMWF, Reading, U.K., 27 pp.

Chevallier, F., P. Bauer, J.-F. Mahfouf, and J.-J. Morcrette, 2002: Variational retrieval of cloud cover and cloud condensate from ATOVS data. *Quart. J. Roy. Meteor. Soc.*, **128**, 2511–2526.

Clough, S., F. Kneizys, and R. Davis, 1989: Line shape and the water continuum. *Atmos. Res.*, **23**, 229–241.

Collard, A. D., and S. B. Healy, 2003: The combined impact of future space-based atmospheric sounding instruments on numerical weather-prediction analysis fields: A simulation study. *Quart. J. Roy. Meteor. Soc.*, **129**, 2741–2760.

Dudhia, A., V. Jay, and C. Rodgers, 2002a: Microwindow selection for high-spectral-resolution sounders. *Applied Optics*, **41**, 3665–3673.

Dudhia, A., P. Morris, and R. Wells, 2002b: Fast monochromatic radiative transfer calculations for limb sounding. *J. Quant. Spectrosc. Radiat. Transfer*, **74**, 745–756.

ESA, 2000: ENVISAT-MIPAS: An instrument for atmospheric chemistry and climate research. ESA report SP-1229, European Space Research and Technology Centre, Noordwijk, The Netherlands, 124 pp.

Eyre, J., 1991: A fast radiative transfer model for satellite sounding systems. Technical Memorandum 176, ECMWF, Reading, UK, 28 pp.

Healy, S., and J. Eyre, 2003: A forward model for the assimilation of GPS radio occultation bending angle measurements. *Quart. J. Roy. Meteor. Soc.*, submitted.

Matricardi, M., 2003: RTIASI-4, a new version of the ECMWF fast radiative transfer model for the infrared atmospheric sounding interferometer. Technical Memorandum 425, ECMWF, Reading, U.K., 63 pp.

Matricardi, M., F. Chevallier, and J.-N. Thépaut, 2004: An improved general fast radiative transfer model for the assimilation of radiance observations. *Quart. J. Roy. Meteor. Soc.*, **130**, 153–173.

Matricardi, M., and R. Saunders, 1999: Fast radiative transfer model for simulation of infrared atmospheric sounding interferometer radiances. *Applied Optics*, **38**, 5679–5691.

Simmons, A. J., and J. K. Gibson, 2000: The ERA-40 project plan. ERA-40 Project Report Series 1, ECMWF, Reading, U.K., 62 pp.